In situ monitoring of the Shikimate pathway: A combinatorial approach of Raman reverse stable isotope probing and hyperspectral imaging.

Jiro Karlo[a], Aryan Gupta[a], Surya Pratap Singh[a]*

[a]Department of Biosciences and Bioengineering, Indian Institute of Technology Dharwad, Dharwad, Karnataka, India.-580011
*Corresponding Author
E.mail: ssingh@iitdh.ac.in

Abstract:

Sensing and visualizing metabolites and metabolic pathways *in situ* for tracking their spatiotemporal dynamics in a non-destructive manner has significant requirement. The shikimate pathway is an important cellular mechanism which leads to the *de novo* synthesis of many compounds containing aromatic rings of high importance such as phenylalanine, tyrosine, and tryptophan. In this work, we present a cost-effective and extraction-free method based on the principles for stable isotope coupled Raman spectroscopy and hyperspectral Raman imaging to monitor and visualize the shikimate pathway activity. We also demonstrated the applicability of this approach for nascent aromatic amino acid localization and tracking turnover dynamics in both prokaryotic and eukaryotic model systems. This method can emerge as a promising tool for both qualitative and semi-quantitative in situ metabolomics, contributing to a better understanding of aromatic ring-containing metabolite dynamics across various organisms.
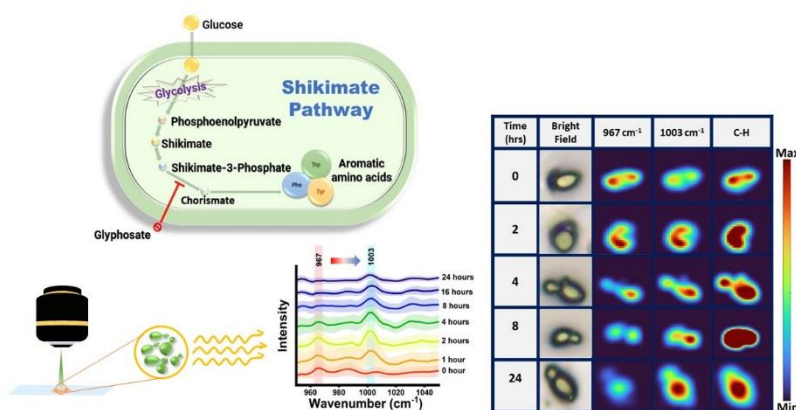
Key words: Raman Spectroscopy, Shikimate pathway, aromatic amino acid biosynthesis, Reverse stable isotope probing, 2D correlation spectroscopy, hyperspectral imaging, multivariate curve resolution, Carbon-13

Introduction:

The shikimate pathway is the bridge between carbon source metabolism and biosynthesis of many aromatic ring-containing metabolites. The major products of this pathways are the three aromatic amino acids i.e. Phenylalanine, Tyrosine and Tryptophan. This pathway is present only in plants and microbes like bacteria and yeast but never in animals. [1,2] The pathway not only secretes aromatic amino acids but many other important aromatic intermediates and aromatic biomolecules such as chorismite, dehydroshikimate, folates, salicylic acid, resveratrol, flavonoids, dopamine, and alkaloids. These molecules have a wide range of applications in developing value-added aromatic compounds for food, agrochemical, fuel additive, cosmetics, dye, pharmaceutical and other industries, Figure 1.[2,3] Over 20% of all the fixed carbon flows through this pathway.[4] Shikimate pathway also plays an important intermediate in the production of antiviral drugs such as oseltamivir.[5] The quinoid core found in benzoquinone and ubiquinone is a derivative of the shikimate pathway in bacteria and yeast.[6] Novel approaches that can help to understand or visualize the metabolites and metabolic pathways *in situ* (in its native position) or *in vivo* (inside the living system) are still in the inception stage. This is primarily attributed to the metabolome complexity and dynamic nature of biomolecules.

The common conventional approaches for metabolite profiling and monitoring metabolic pathways are gas chromatography-mass spectrometry and liquid chromatography-mass spectrometry (GC-MS and LC-MS). [4–8] These are highly efficient and sensitive methods for both qualitative and quantitative analysis of the entire pathway at each step till the final product. However, these approaches require the extraction of the metabolites and does not provide information related to the dynamic nature of metabolic pathway.[7,8] Fluorescence spectroscopy-based methods are an alternative, but it involves introduction of foreign molecules which can perturb the natural metabolic process.[7] Raman spectroscopy is an efficient label-free, reagent-free, and non-destructive analytical tool for analysing biomolecules *in situ*. Stable isotope probes such as ^{2}H, ^{13}C, ^{15}N, and ^{18}O can be used as tags for analysing the *de novo* biosynthesis of different biomolecules simultaneously using Raman spectroscopy. When the parent atom is replaced by its heavier isotope the reduced mass increases. As the
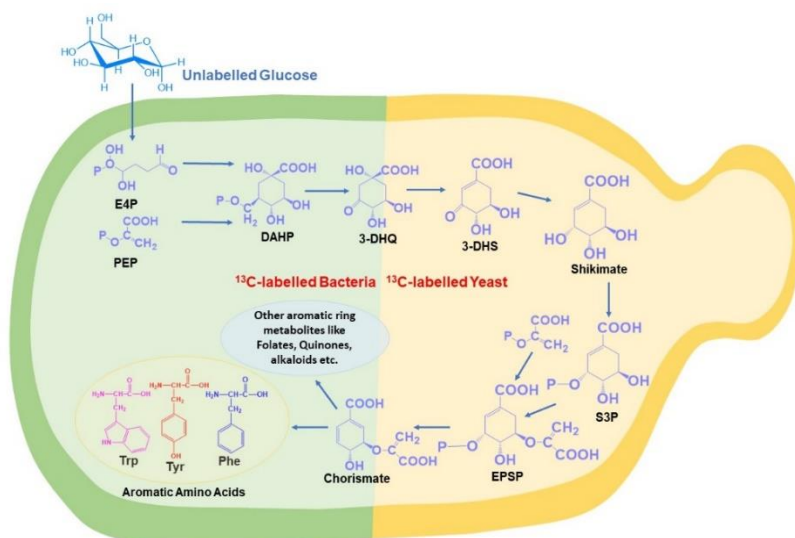
Fig. 1 Shikimate pathway in Bacteria and Yeast showing the carbon flow from unlabelled glucose. (Abbreviation: E4P - Erythrose 4-Phosphate; PEP – Phosphoenol pyruvate; DAHP – 3-Deoxy-o-arabino-heprulosonate 7-phosphate; 3-DHQ – 3-Dehydroxyquinate; 3-DHS – 3-Dehydroshikimate; S3P – Shikimate 3-Phosphate; EPSP – 5-Enolpyruvylshikimate 3-phosphate; Phe – Phenylalanine; Tyr – Tyrosine; Trp – Tryptophan)

relationship between the wavenumber and the square root of reduced mass is not directly proportional, due to this isotopic effect, the wavenumber shifts to a lesser wavenumber known as the redshift of the peak. However, this approach is limited by the fact that the stable isotope sources are not abundantly available the relative cost is higher when compared to its unlabelled counterpart. To overcome this, we have used the strategy of Raman reverse stable isotope probing (RrSIP). A reverse isotopic effect is seen where the heavier isotope is replaced by the lighter isotope resulting in a reduction of reduce mass and a shift towards a higher wavenumber (blue shift) [9–11].

In this study, for the first time, we report *in situ* monitoring of shikimate pathway activity at a community level in *Escherichia coli* (prokaryotic microbe) and single-cell level in *Saccharomyces cerevisiae* (eukaryotic microbe). The primary reason for using these two model systems is their well-known utility in industrial fermentation and a wide range of biotechnological applications. We are reporting visualization of shikimate pathway activity *via* sensing the spatial distribution of nascent phenylalanine peak through hyperspectral Raman imaging combined with RrSIP with time. We also performed multivariate Curve Resolution (MCR) to extract each component with interpretable spectra from a complex mixture of spectral data. This approach of Raman spectroscopy and imaging combined with RrSIP can be a promising analytical tool to explore different metabolic pathways involving aromatic rings.

Results and Discussion

In situ sensing the shikimate pathway activity and monitoring *de novo* synthesis of Phenylalanine using Raman spectroscopy.
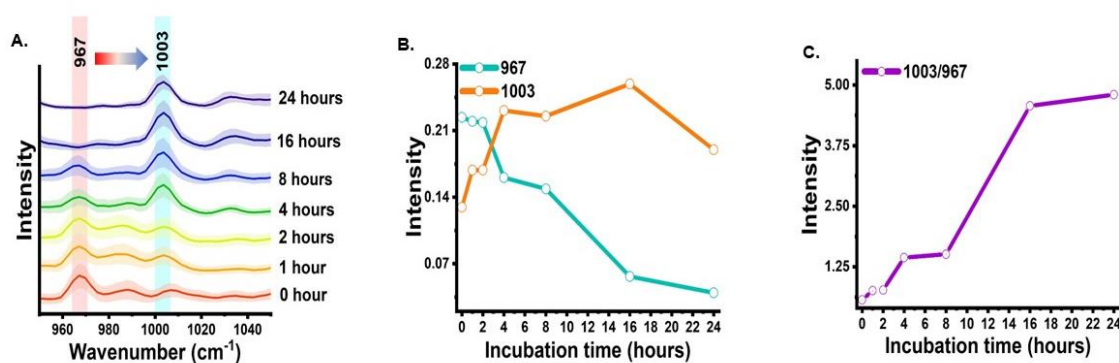

Fig. 2 Time dependent sensing the shikimate pathway activity using representative peak as Phenylalanine using RrSIP. (A) Mean Raman spectra with standard deviation of *E. coli* at a specific range showing blue shift of Phenylalanine peak from 967 cm^{-1} toward 1003 cm^{-1} with time. (B) Intensity plot showing incorporation of ^{13}C in newly synthesized phenylalanine. (C) Intensity ratio plot showing the turnover of nascent phenylalanine replacing the old pool of Phenylalanine with time**.**

The shikimate pathway is directly related to the biosynthesis of aromatic amino acids. Therefore, Phenylalanine was taken as the Raman representative signature peak. It shows a strong unique peak in Raman spectra of cells at 1003 cm^{-1} for unlabelled phenylalanine and 967 cm^{-1} for ^{13}C labelled phenylalanine, Table 1. This peak arises due to the ring-breathing vibration. In Raman reverse stable isotope probing

approach the ^{13}C labelled *E. coli* is allowed to grow in unlabelled media and Raman spectra of the cells at various time points at 0-, 1-, 2-, 4-, 8-, 16- and 24-hours post-incubation are acquired, Figure 2(A). Initially, at 0-hour the peak intensity of 967 cm^{-1} is high and very low at 1003 cm^{-1}. This indicates that nearly the entire aromatic amino acid pool inside cells is ^{13}C labelled. However, with the increase in the incubation time, we observe dynamic changes in the peak intensity. The peak at 967 cm^{-1} gradually decreases and simultaneously there is a gradual increase in peak intensity at 1003 cm^{-1}. At 1 and 2 hours we observe a small signal at 1003 cm^{-1}, this blue shift in the phenylalanine peak indicates the incorporation of ^{12}C in the newly synthesized phenylalanine from the supplemented unlabelled glucose which suggests the positive shikimate pathway activity in the *E. coli* cells. At 4 hours post-incubation, we observed that the intensity of both bands is nearly equal. At the later time points at 8, 16 and 24 hours a significant decrease in the 967 cm^{-1} peak intensity and an exponential increase in the peak intensity at 1003 cm^{-1} can be observed. This blue-shift of peak with time can be interpreted as the old pool of aromatic amino acids moderately getting substituted by the newly synthesised aromatic amino acids *via* the active shikimate pathway in the cells. This can be better visualized in the line plot shown in Figure 2(B) and 2(C). It represents a dynamic intensity *vs* time plot showing the incorporation of ^{12}C in the Phenylalanine pool of the cell. This enables us to track the carbon flows from the supplement carbon source to the aromatic amino acid through the Shikimate pathway. The time-dependent change in the ratiometric intensity of 1003/967 cm^{-1} is plotted in Figure 2(C) which shows the turnover of the nascent unlabelled phenylalanine in the cell.

The next analysis was to establish and validate that the origin of the blue-shifted phenylalanine reference peak is via the shikimate pathway only. To achieve this, we have monitored the growth of cells with and without glyphosate treatment. Glyphosate (N-[Phosphonomethyl]-glycine) is a well-known inhibitor of the shikimate pathway in *E. coli*. [12,13] To check the inhibitory action of glyphosate, OD_{600} values from the treated culture were plotted against the incubation time as shown in Figure S1. Post-treatment, we can see that the OD_{600} values do not increase with the incubation time confirming the inhibitory effect of glyphosate on the phenylalanine synthesis of *E. coli*. Post-treatment Raman spectra from the cells were recorded at time points 0, 1, 2, 4, 8, 16 and 24 hours post incubation are shown Figure 3 (A). As can be seen the blue shift of the Phenylalanine peak has stopped due to the disruption in the shikimate pathway activity. There are negligible changes in peak intensity at 1003 cm^{-1} with the increase in incubation times which was expected to be coming from the nascent phenylalanine when compared against the peak intensity of the untreated group shown in Figure 2 (A). This observation suggests that the assigned peak at 1003 cm^{-1} has its origin indeed from the shikimate pathway activity.
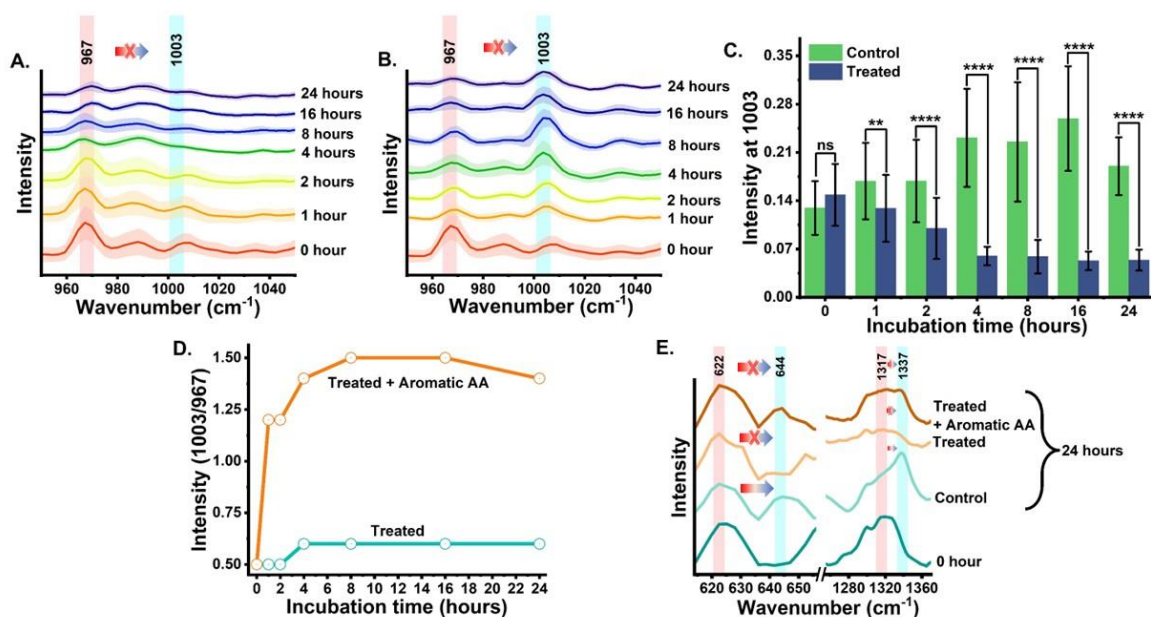

Fig. 3 Validating the peak from the nascent aromatic amino acid in *E. coli*. (A) Time dependent mean Raman spectra with standard deviation of *E. coli* treated with glyphosate. (B) Time dependent mean Raman spectra with standard deviation of glyphosate treated *E. coli* supplemented with exogenous aromatic amino. (C) Intensity bar plot at 1003 cm^{-1} of control versus treated group showing statistical significance {ns ($p > 0.05$), * ($p \leq 0.05$),** ($p \leq 0.01$), *** ($p \leq 0.001$),**** ($p \leq 0.0001$)}. (D) Intensity line plot at 1003 cm^{-1} of glyphosate treated group vs aromatic amino acid supplemented glyphosate treated group. (E) Mean Raman spectra at 0 hour and 24 hours showing blueshift of Tyrosine and Tryptophan peaks in different treatment condition at 0 and 24 hours.

Further, we also performed a complementary analysis by reversing the inhibitory effect of glyphosate on the shikimate pathway of the cells. The glyphosate-treated growth medium was exogenously supplemented with the three unlabelled aromatic amino acids that are essential for cell survivability. The Raman spectra of all three supplemented unlabelled aromatic amino acids were recorded (Figure S3) to ensure the purity and peaks of interest. The Raman spectra from the cells were recorded at various time points at 0, 1, 2, 4, 8, 16 and 24 hours as shown in Figure 3(B). We successfully monitored the incorporation of exogenous aromatic amino acids from the growth media in the glyphosate-

treated cells with Raman spectroscopy in an extraction-free manner. At 1 hour we notice a rapid increment of intensity at 1003 cm^{-1} when compared to untreated cells. However, with the incubation time, it increases gradually. It was seen that this increase in the peak at 1003 cm^{-1} was not accompanied by the diminishing signal at the 967 cm^{-1} peak signal at 1 hour and so on. It confirms that there is no blue shift in the Phenylalanine band confirming the inhibited Shikimate pathway, but the signal at 1003 cm^{-1} is from supplemented phenylalanine. This validates the fact that *de novo* synthesized or exogenously supplied, the peak at 1003 cm^{-1} from the cell is indeed derived from the unlabelled phenylalanine only. Furthermore, to verify the statistical significance of the Raman intensity difference between treated and untreated cell groups for nascent phenylalanine at 1003 cm^{-1} peak we have performed a student's t-test (Welch corrected). In Figure 3(C) the significance (p-value ≤ 0.05) of the intensity difference can be observed from the 1 hour of incubation time. Likewise, the dynamic ratio metric intensity difference was calculated as seen in line plot Figure 3(D) for the treated and treated supplemented with the aromatic amino acid group.

Table 1. Band assignment for biomolecular bonds associated with shikimate pathway sensing.

^{13}C labelled (cm^{-1})	Unlabelled (cm^{-1})	Assignment	Significance	Ref.
622	644	Tyrosine	622 is overlapped by unlabelled Phenylalanine and ^{13}C-labelled Tyrosine. Possible qualitative marker	14–17
967	1003	Phenylalanine	Evident qualitative and quasi-quantitative marker	11,14–16,18–20
1317	1337	Tryptophan	Band overlap by Adenine and Guanine. Possible Qualitative marker	14–16

Tracking the shikimate pathway dynamics using Tyrosine and Tryptophan Raman spectral markers and 2D Correlation spectroscopy

The phenylalanine position is known to be represented by a sharp single peak.[14] Therefore, Phenylalanine peaks at 967 and 1003 cm^{-1} can act as both qualitative and quasi-quantitative markers for studying the Shikimate pathway dynamics in a non-destructive manner. In addition to this, peaks assigned to other major products of the shikimate pathway such as tyrosine and tryptophan can also act as qualitative markers as shown in Figure 3(E). These peaks cannot be preferred for semi-quantitative analysis as it is influenced by other biomolecular Raman bands as shown in Table 1. In the previous studies, the peak at around 622 and 1317 cm^{-1} has been assigned to ^{13}C labelled tyrosine and tryptophan whereas the peak at around 644 and 1337 cm^{-1} has been assigned to unlabelled tyrosine and tryptophan as shown in Table 1. [14,16] At 0 hour we observe that intensified signal at 622 and 1317 cm^{-1} but negligible intensity at 644 and 1337 cm^{-1}. However, after 24 hours of incubation, we observe an intensified signal from the new peak at 644 and 1337 cm^{-1} giving us insight to the active shikimate pathway qualitatively. Unlike ^{13}C-labelled Phenylalanine peaks, ^{13}C-labelled tyrosine and tryptophan peaks do not change much. This is because during the reverse labelling process the 622 cm^{-1} band is also overlapped by the newly synthesized unlabelled phenylalanine. Likewise, the 1317 cm^{-1} band is contributed by other biomolecular bands such as adenine and guanine, Table 1. Furthermore, the inhibition of the shikimate pathway by glyphosate treatment also shows a negative effect on the blue shift of these bands and the supplement of aromatic amino acid
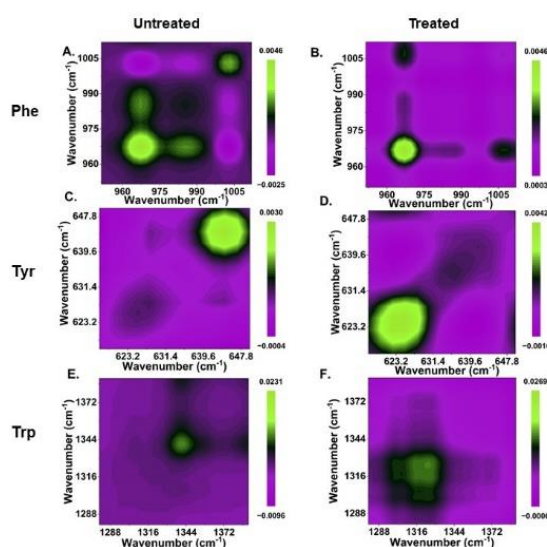

Fig. 4 Two-dimensional Synchronous correlation map of Untreated and Treated cells (A,B) Phenylalanine; (C,D) Tyrosine; (E,F) Tryptophan. Each Map includes mean Raman spectra of different incubation time points to provide the spectral dynamics over the perturbation range. The fluorescent green peaks are positive and magenta peaks are negative.

exogenously shows the reversal effect. This further confirms tyrosine and tryptophan can also act as evident qualitative Raman spectral markers for monitoring the shikimate pathway *in situ*.

Further to resolve and validate the time-dependent overlapping Raman peak dynamics, we performed a two-dimensional correlation analysis. The synchronous correlation map was generated from the mean Raman spectra of various time points as shown in Figure 4. The auto peak along the diagonal corresponds to the dynamics of that peak with time. We observe a strong auto peak in the correlation map of the untreated group at the unlabelled position of nascent phenylalanine, tyrosine, and tryptophan. This corresponds to the fact that these peaks have changed over time which is due to the active shikimate pathway resulting in turnover of nascent aromatic acid. In contrast, we observed in the treated group a strong auto peak at 1004, 1317 and 622 cm^{-1} which supports that the ^{13}C labelled peak has gone through significant changes with time. Furthermore, we observed a negative cross peak for ^{13}C labelled and an unlabelled aromatic amino acid peak position in the untreated group. This shows the negative correlation between two peak positions that is the dynamics are in opposite directions which supports the fact of shikimate pathway activity in cells.

***In situ* monitoring and visualization of *de novo* Phenylalanine synthesis at the single cell level in the eukaryotic system**
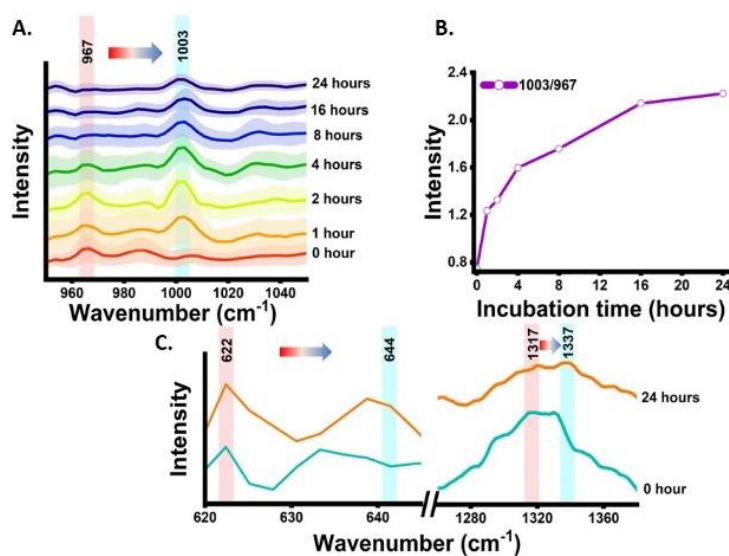
After

Fig. 5 Time dependent sensing the shikimate pathway activity using representative peak as Phenylalanine using RrSIP. (A) Mean Raman spectra with standard deviation of Single *S. cervesiae* cell at a specific range showing blue shift of Phenylalanine peak from 967 cm^{-1} toward 1003 cm^{-1} with time. (B) Ramanometry intensity ratio plot showing the turnover of nascent phenylalanine replacing the old pool of Phenylalanine with time in single *S. cervesiae* cell. (C) Mean Raman spectra showing blueshift of Tyrosine and Tryptophan peaks at 0 and 24 hours.

demonstrating the potentials of Raman spectroscopy in monitoring shikimate pathway activity using nascent phenylalanine peak dynamics at 1003 cm^{-1} at the community level in microbes, we monitored the shikimate pathway at single cell level using *Saccharomyces cerevisiae* by employing the same reverse stable isotope probing strategy. Raman Spectra were recorded from the single yeast cell at various incubation time points of 0, 1, 2, 4, 8, 16 and 24 hours as shown in Figure 5(A). At the initial time point, the 967 cm^{-1} peak intensity was high while the intensity was low for 1003 cm^{-1}, indicating a ^{13}C labelled aromatic amino acid pool inside the cells. Over time, we observed that the peak at 1003 cm^{-1} intensifies through the blue shift of 967 cm^{-1}. This temporal shift implies that Raman spectroscopy can sense the positive shikimate pathway activity at the single-cell level and the gradual turnover of nascent phenylalanine replacing the older pool of phenylalanine can be objectively monitored. The time-dependent increase in the ratio metric intensity plot depicted in Figure 5(B) illustrates the incorporation of ^{12}C in the nascent phenylalanine and the relative turnover process over time at the single-cell level. Further, we monitored the qualitative spectral marker of shikimate pathway dynamics which is the peak assigned to tyrosine and tryptophan as shown in Figure 5(C). At 0 hours we observe negligible peak intensity at 644 cm^{-1} and low peak intensity at 1337 cm^{-1}. However, at 24 hours we observe an intensified signal from the peak suggesting the turnover of the shikimate pathway synthesized tyrosine and tryptophan with time.

Raman hyperspectral imaging combines spectroscopy with imaging which provides information not only about the biomolecular components but also its spatial distribution with subcellular resolution at different pixel positions of the Raman image. We mapped the peak intensity of phenylalanine at 967 and 1003 cm^{-1} from the single *S cerevisiae* cell taken from various time points at 0, 2, 4, 8 and 24 hours as shown in Figure 6 (A). Time points for Raman imaging were decided by analysing the notable change in the mean Raman spectra of the single cell as shown in Figure 5(A). The bright field and corresponding Raman image of the C-H band show the cellular boundary. The Raman image of the cell at 0 hours shows a highly intensified image at 967 cm^{-1} with respect to 1003 cm^{-1} indicating the initial phenylalanine pool to be ^{13}C labelled. This distribution of phenylalanine comes from the free phenylalanine from the cytoplasm as well as the protein structures. The Raman image of the cell at 2 hours post inoculation shows the nearly equivalent spatial intensity distribution of the phenylalanine at 967 and 1003 cm^{-1}. This confirms the positive shikimate pathway activity and nearly equivalent distribution of the ^{13}C labelled and unlabelled

phenylalanine in the cellular phenylalanine pool as shown in the mean Raman spectra from a single cell in Figure 5(A). Likewise, with the increase in the incubation time, we see the spatial distribution of the ^{13}C labelled phenylalanine diminish while that of the unlabelled nascent phenylalanine increases confirming the visualisation of the phenylalanine turnover dynamics. We also noticed the newly formed bud of the budding yeast shows intensified 1003 cm^{-1} giving insight into carbon flow and newly synthesized aromatic amino acids in the bud connected to the mother cell. The Raman image was constructed targeting the distribution of single peak intensity in each pixel. Multivariate curve resolution (MCR) was performed to resolve the complex mixture of spectral data of the Raman image into various components by conserving the chemical meaning in each component. We observed that the two components had most of the information of interest for understanding the biomolecular spectral pattern. For quenching out the biomolecular Raman spectral pattern from the mixed complex hyperspectral Raman data MCR analysis with two components was performed. Among the two MCR components under study, one component had the phenylalanine and other biomolecular information of the cell of our interest and the other one has a negligible interpretable biomolecular spectral pattern which consists of background information as shown in Figure 6(B). MCR 1 component map at various time points showed a similar cell boundary and pattern when compared to bright field images shown in Figure 6(A). The corresponding MCR1 component loading plot can be seen with phenylalanine peak intensity marked in Figure 6(B). We can see the dynamics in the phenylalanine band at 967 cm^{-1} and 1003 cm^{-1} with time at single cell level.
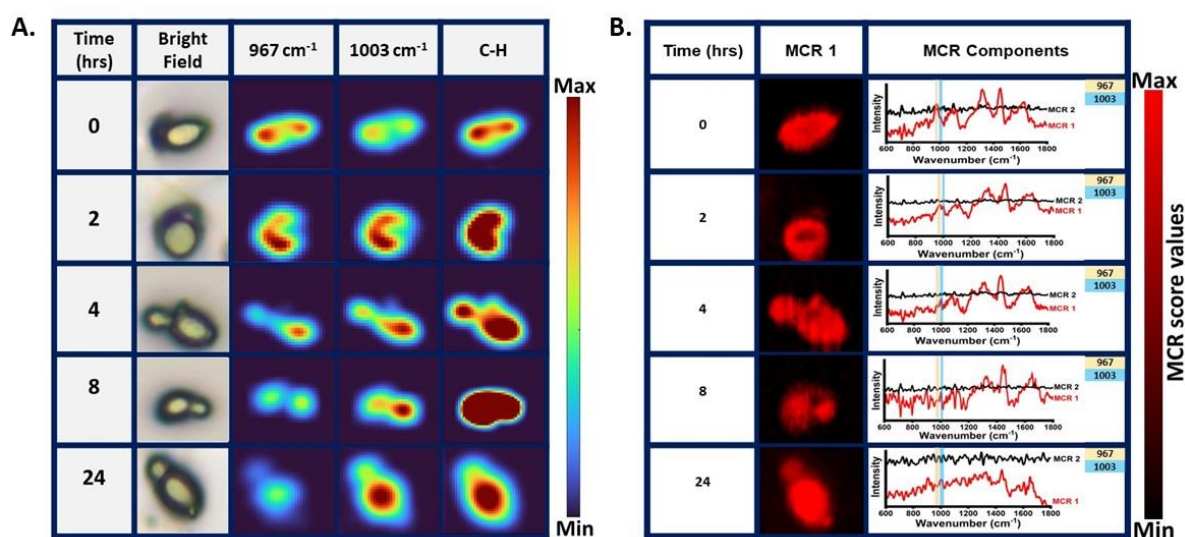

Fig. 6 (A) Raman Single cell level visualization of phenylalanine turnover and shikimate pathway activity with incubation time in Yeast cell showing Bright field image for reference and corresponding Raman image at 967 cm^{-1} (^{13}C labelled Phenylalanine) , 1003 cm^{-1} (Unlabelled nascent Phenylalanine) and CH stretch (defining Raman image cell boundary). (B) Raman image constructed from Multivariate Curve Resolution analysis for MCR 1 and corresponding loading plots of MCR components in the bio-fingerprint region from 600 to 1800 cm^{-1} showing blue shift in phenylalanine band with time in MCR 1 component.

Overall findings suggest that Raman spectroscopy and hyperspectral imaging combined with reverse stable isotope probing could serve as an extraction-free and non-destructive approach for metabolic pathway monitoring. Previously, Weng J et al have reported high single-cell phenotypic heterogeneity of carbon uptake and hydrogen uptake in carotenoids using Raman stable isotope probing (RSIP).[21] Li J et al using Raman active cell sorting SIP identified, sorted and isolated the active toluene degrader single cell *Pigmentiphaga.*[22] Li Menqui et al have shown the potential of RSIP using phenylalanine and thymine as Raman spectral biomarkers to track the carbon flow in predator-prey model at the single cell level. [19] Although these studies explored the possibilities of RSIP, we considered RrSIP as a cost-effective approach with respect to RSIP, as preparing the labelled cell for inoculation, and growing in unlabelled media will require an extremely low amount of stable isotope. Additionally, employing RrSIP reveals a blue shift in the Raman spectra, signifying the migration of labelled metabolite peaks toward the position of unlabelled metabolite peaks over time. This shift can be readily confirmed, as the positions of unlabelled bands in the cell spectra have been thoroughly investigated in previous studies. [11,20] In one of our recent studies we have reported the utility of this approach for global proteome monitoring.[11] Due to the easy availability and low cost of unlabelled supplements, it is an efficient approach to work in large growth medium volume requirements. This offers an attractive opportunity in future for sensing and visualizing metabolites and metabolic pathways inside the cell in situ or in vivo. As cell has carbon everywhere at the genome, proteome, and metabolome level, carbon-based RrSIP can give insight into sensing the *de novo* synthesis and turnover of different metabolites without any requirement of extraction. In our work, we have described its potential in prokaryotic and eukaryotic model systems. A remarkable finding in this work is the observation that the phenylalanine peak at 967 and 1003 cm^{-1} is established as a Raman metabolic spectral marker for studying the shikimate pathway activity, *de novo* phenylalanine synthesis, and the turnover dynamics of nascent phenylalanine over time. We have verified that the signal arising from newly synthesized unlabelled phenylalanine originated solely from the shikimate pathway *via* an inhibition assay and bypassing the effect of inhibition with exogenous supplements.

One of the multiple beneficial attributes of this approach is that along with the 1D temporal spectral information, spatial information can also be derived using Raman hyperspectral imaging. It provides an image representation of the sample with different pseudo-colours

corresponding to the intensity of the biomolecular peak for visualization and quantification. Along with the identification it also gives information about the heterogeneity of the scanned area without the requirement of endogenous and exogenous labels or markers, unlike the conventional fluorescence-based method. The endogenous labels like fluorescent protein and exogenous labels like dyes (Nile red, BIODPY) or quantum dots can interfere with the metabolic activity or can cause photobleaching or phototoxicity. [7,23–28] Raman hyperspectral imaging combined with multivariate curve resolution validates the sensitivity and specificity of our approach. Visualizing the spatial distribution and extracting the spectral pattern of phenylalanine from intricate spectral data not only contributes to the validation of our study but also enhances our ability to explore shikimate pathway activity at various incubation times in situ. Furthermore, we have identified peak positions linked to tyrosine and tryptophan, serving as potential qualitative markers. This identification has been further corroborated through the application of two-dimensional correlation spectroscopy, adding validation to our findings.

Experimental

Microbial rSIP culture conditions and sample preparation

In our study, the bacterial strain *Escherichia coli* K12 and yeast strain *Saccharomyces cerevisiae* was used. For the primary culture, a single colony was inoculated into a carbon-free growth medium with 5g/L of uniformly labelled ^{13}C glucose (Cambridge Isotope Laboratories), as the sole carbon source. This secondary broth culture was incubated overnight according to standard microbial culture protocol. Aliquot of the ^{13}C-labeled *microbial* cells was taken and centrifuged at 7000g. Subsequently, the cells were subjected to two washes with phosphate-buffered saline (PBS, Sisco Research Laboratories) to eliminate any residual traces of the ^{13}C-labelled growth medium. Immediately after the washing steps, the cell pellets were reintroduced into growth medium, this time with 5g/L of unlabelled (^{12}C) glucose (Sigma-Aldrich) as the exclusive carbon source. This culture was then subjected to standard incubation protocols. An inhibition assay was conducted using Glyphosate, a well-known shikimate pathway inhibitor (Sigma-Aldrich). A working concentration of 700 µg/ml Glyphosate concentration was introduced to M9 minimal media containing 5g/L unlabelled carbon before inoculating the ^{13}C labelled cells.[29] Following a similar procedure along with the mentioned glyphosate treatment, a supplement of three aromatic amino acids with 30 µg/ml was added in the growth medium. Subsequently, growth monitoring experiments were performed for all culture using the optical density method at 600 nm (OD$_{600}$). Values were recorded at various time points starting initially at 0 hour till 24 hours as shown in Figure S1 and S2.

Raman spectra measurement and analysis

Aliquots of microbial samples were collected from both controls and treated groups at various time intervals, 0, 1, 2, 4, 8, 16 and 24 hours. Appropriate dilutions were performed to maintain approximately equal number of cells. The sample was immediately centrifuged at 7000 rpm for 5 mins, followed by two washes with PBS. Similar procedure was performed with yeast samples. The cells were kept on the clean and ethanol-washed slide and Raman Spectra were acquired using WITec Confocal micro-Raman spectrometer, equipped with a 532 nm laser source, 100x objective with a numerical aperture of 0.8. Single spectrum was averaged over 5 accumulations with 10-second exposure time in the spectral range of 200 to 3200 cm^{-1} with 600 gr/mm diffraction grating. The Raman spectral data was pre-processed using MATLAB R2021B. Smoothening was applied using the Savitzky Golay filter, 5th order polynomial was used for baseline correction and unit normalization was done. All spectral plots and figures were generated using Origin Pro 2023b.

Single cell Raman imaging and MCR analysis

For the Raman imaging yeast cells were collected in the similar procedure mentioned earlier. The cells were diluted to an optimized concentration to make sure single cells can be obtained from the cell pellet. After dilution, 10 µl was spread on an ethanol washed Calcium fluoride substrate and it was subjected to Raman imaging using above mentioned WITec Confocal micro-Raman spectrometer. The step size of the scan was kept at 0.33 microns with 5 sec laser exposure time. The Raman hyperspectral data were pre-processed, and the Raman image was generated using in-house scripts in MATLAB 2021B software. Multivariate curve resolution analysis (MCR) was done using RamApp.[30] MCR analysis was initiated to resolve the complex spectral matrix into two components while these two MCR components retain the interpretable spectral information.

Conclusions:

Overall, the findings of our study demonstrate the immense potentials of this combinatorial approach in objectively unravelling the dynamics and complexities of metabolic pathways. The presented approach is cost effective and has potentials to be translated into a preferred approach for monitoring the production of commercially or medically relevant metabolites and byproducts.

Conflicts of interest

 "There are no conflicts to declare".

Acknowledgements

References

1   K. M. Herrmann and L. M. Weaver, THE SHIKIMATE PATHWAY, *Annu Rev Plant Physiol Plant Mol Biol*, 1999, **50**, 473–503.

2   H. Liu, Q. Xiao, X. Wu, H. Ma, J. Li, X. Guo, Z. Liu, Y. Zhang and Y. Luo, Mechanistic investigation of a D to N mutation in DAHP synthase that dictates carbon flux into the shikimate pathway in yeast, *Commun Chem*, 2023, **6**, 152.

3   J.-H. Lee and V. F. Wendisch, Biotechnological production of aromatic compounds of the extended shikimate pathway from renewable biomass, *J Biotechnol*, 2017, **257**, 211–221.

4   K. M. Herrmann, The Shikimate Pathway: Early Steps in the Biosynthesis of Aromatic Compounds., *Plant Cell*, 1995, **7**, 907–919.

5   H.-N. Lee, S.-Y. Seo, H.-J. Kim, J.-H. Park, E. Park, S.-S. Choi, S. J. Lee and E.-S. Kim, Artificial cell factory design for shikimate production in Escherichia coli., *J Ind Microbiol Biotechnol*, , DOI:10.1093/jimb/kuab043.

6   R. Meganathan, Ubiquinone biosynthesis in microorganisms, *FEMS Microbiol Lett*, 2001, **203**, 131–139.

7   C. Lima, H. Muhamadali and R. Goodacre, The Role of Raman Spectroscopy Within Quantitative Metabolomics, *Annual Review of Analytical Chemistry*, 2021, **14**, 323–345.

8   J. Karlo, R. Prasad and S. P. Singh, Biophotonics in food technology: Quo vadis?, *J Agric Food Res*, 2023, **11**, 100482.

9   Y. Wang, W. E. Huang, L. Cui and M. Wagner, Single cell stable isotope probing in microbiology using Raman microspectroscopy, *Curr Opin Biotechnol*, 2016, **41**, 34–42.

10   Y. Wang, W. E. Huang, L. Cui and M. Wagner, Single cell stable isotope probing in microbiology using Raman microspectroscopy, *Curr Opin Biotechnol*, 2016, **41**, 34–42.

11   J. Karlo, A. K. Dhillon, S. Siddhanta and S. P. Singh, Reverse stable isotope labelling with Raman spectroscopy for microbial proteomics, *J Biophotonics*, , DOI:10.1002/jbio.202300341.

12   D. Patriarcheas, T. Momtareen and J. E. G. Gallagher, Yeast of Eden: microbial resistance to glyphosate from a yeast perspective, *Curr Genet*, 2023, **69**, 203–212.

13   B. Ely and J. Pittard, Aromatic amino acid biosynthesis: regulation of shikimate kinase in Escherichia coli K-12., *J Bacteriol*, 1979, **138**, 933–43.

14   F. Weber, T. Zaliznyak, V. P. Edgcomb and G. T. Taylor, Using Stable Isotope Probing and Raman Microspectroscopy To Measure Growth Rates of Heterotrophic Bacteria, *Appl Environ Microbiol*, , DOI:10.1128/AEM.01460-21.

15   F. S. de Siqueira e Oliveira, H. E. Giana and L. Silveira, Discrimination of selected species of pathogenic bacteria using near-infrared Raman spectroscopy and principal components analysis., *J Biomed Opt*, 2012, **17**, 107004.

16   S. Sil, R. Mukherjee, N. S. Kumar, A. S., J. Kingston and U. K. Singh, Detection and classification of Bacteria using Raman Spectroscopy Combined with Multivariate Analysis, *Def Life Sci J*, 2017, **2**, 435.

17   C. Fan, Z. Hu, A. Mustapha and M. Lin, Rapid detection of food- and waterborne bacteria using surface-enhanced Raman spectroscopy coupled with silver nanosubstrates, *Appl Microbiol Biotechnol*, 2011, **92**, 1053–1061.

18   J. Karlo, A. K. Dhillon, S. Siddhanta and S. P. Singh, Monitoring of microbial proteome dynamics using Raman stable isotope probing, *J Biophotonics*, , DOI:10.1002/jbio.202200341.

19   M. Li, W. E. Huang, C. M. Gibson, P. W. Fowler and A. Jousset, Stable Isotope Probing and Raman Spectroscopy for Monitoring Carbon Flow in a Food Chain and Revealing Metabolic Pathway, *Anal Chem*, 2013, **85**, 1642–1649.

20   Y. Wang, Y. Song, Y. Tao, H. Muhamadali, R. Goodacre, N.-Y. Zhou, G. M. Preston, J. Xu and W. E. Huang, Reverse and Multiple Stable Isotope Probing to Study Bacterial Metabolism and Interactions at the Single Cell Level, *Anal Chem*, 2016, **88**, 9443–9450.

21   J. Weng, K. Müller, O. Morgaienko, M. Elsner and N. P. Ivleva, Multi-element stable isotope Raman microspectroscopy of bacterial carotenoids unravels rare signal shift patterns and single-cell phenotypic heterogeneity, *Analyst*, 2023, **148**, 128–136.

22   J. Li, D. Zhang, C. Luo, B. Li and G. Zhang, In Situ Discrimination and Cultivation of Active Degraders in Soils by Genome-Directed Cultivation Assisted by SIP-Raman-Activated Cell Sorting, *Environ Sci Technol*, 2023, **57**, 17087–17098.

23   D. Fu, Quantitative chemical imaging with stimulated Raman scattering microscopy, *Curr Opin Chem Biol*, 2017, **39**, 24–31.

24   G. Barzan, A. Sacco, L. Mandrile, A. M. Giovannozzi, C. Portesi and A. M. Rossi, Hyperspectral Chemical Imaging of Single Bacterial Cell Structure by Raman Spectroscopy and Machine Learning, *Applied Sciences*, 2021, **11**, 3409.

25   M. Hosokawa, M. Ando, S. Mukai, K. Osada, T. Yoshino, H. Hamaguchi and T. Tanaka, In vivo live cell imaging for the quantitative monitoring of lipids by using Raman microspectroscopy., *Anal Chem*, 2014, **86**, 8224–30.

26   C. Kallepitis, M. S. Bergholt, M. M. Mazo, V. Leonardo, S. C. Skaalure, S. A. Maynard and M. M. Stevens, Quantitative volumetric Raman imaging of three dimensional cell cultures, *Nat Commun*, 2017, **8**, 14843.

27   H. Noothalapati, T. Sasaki, T. Kaino, M. Kawamukai, M. Ando, H. Hamaguchi and T. Yamamoto, Label-free Chemical Imaging of Fungal Spore Walls by Raman Microscopy and Multivariate Curve Resolution Analysis, *Sci Rep*, 2016, **6**, 27789.

28   H. Noothalapati, K. Iwasaki and T. Yamamoto, Biological and Medical Applications of Multivariate Curve Resolution Assisted Raman Spectroscopy, *Analytical Sciences*, 2017, **33**, 15–22.

29   V. Ramachandran, V. Ramachandran, R. Singh, S. Yang, T. Ragadeepthi, S. Mohapatra, S. Khandelwal and S. Patel, Genetic and chemical knockdown: a complementary strategy for evaluating an anti-infective target, *Advances and Applications in Bioinformatics and Chemistry*, 2013, 1.

30   Renzo Vanna, Giulia De Poli, Andrea Masella, Elia Broggio, Dario Polli and Matteo Bregonzio, RamApp.
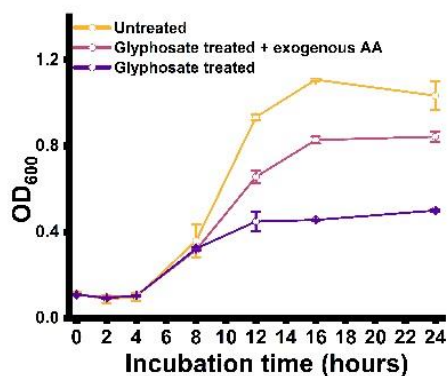
Supplementary Figures:

Fig. S1 Growth curve of *E. coli* grown in M9 minimal medium, Glyphosate treated medium, Glyphosate treated medium supplemented with exogenous Aromatic Amino acids.
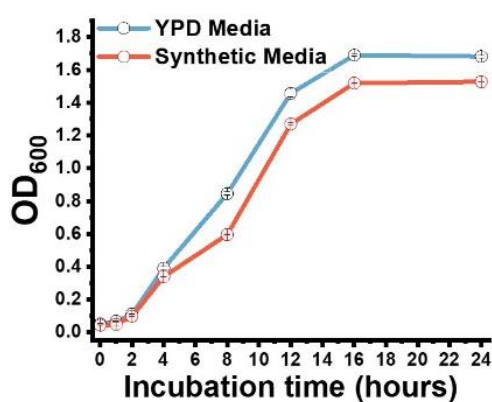

Fig. S2 Evaluating the feasibility of Synthetic media with glucose as only carbon source for the growth of S. cerevisiae.
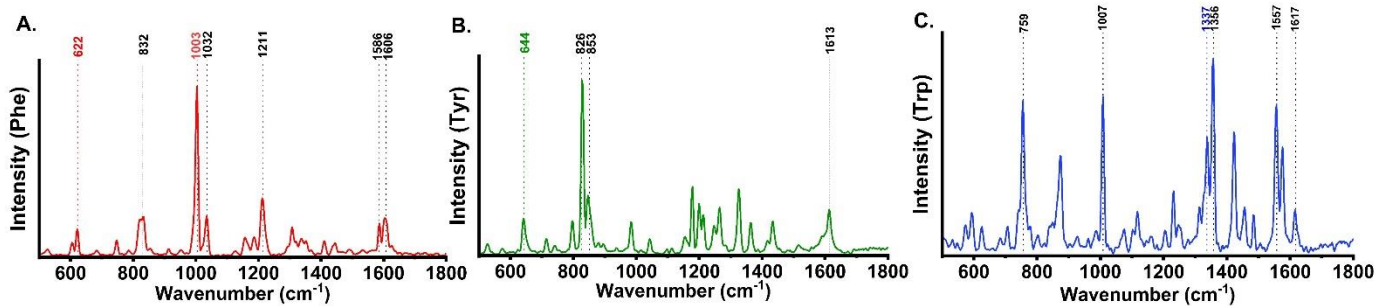

Fig. S3 Mean Raman spectra of supplemented exogenous aromatic amino acid and the corresponding reference bands are marked in colours. (A) Phenylalanine (B) Tyrosine (C) Tryptophan.